Supporting Information

for

Effective one-pot multienzyme (OPME) synthesis of monotreme milk oligosaccharides and other sialosides containing a 4-*O*-acetyl sialic acid

Hai Yu,‡[a] Jie Zeng,‡[a,b] Yanhong Li,[a] Vireak Thon,§[a] Baojun Shi,[a,c] and Xi Chen*[a]

[a]*Department of Chemistry, University of California, One Shields Avenue, Davis, CA 95616, USA. E-mail: xiichen@ucdavis.edu; Fax: +1 530 752-8995; Tel: +1 530 754-6037*

[b]*School of Food Science, Henan Institute of Science and Technology, Xinxiang, Henan 453003, China*

[c]*College of Plant Protection, Northwest A&F University, Yangling, Shaanxi 712100, China*

‡These authors contributed equally to this work

§Current address: Laboratory of Bacterial Polysaccharides, Food and Drug Administration, Bethesda, MD 20892, USA.

*Corresponding author. E-mail: xiichen@ucdavis.edu; Fax: +1 530 752-8995; Tel: +1 530 754-6037

Table of Contents

Fig. S1 Mass spectrometry (MS) chromatograms of reactions catalyzed by various bacterial CMP-sialic acid synthetases (CSSs) and mutants. Reactions were performed in a total volume of 10 μL containing Tris-HCl buffer (100 mM, pH 7.1), $MgCl_2$ (20 mM), $Neu4,5Ac_2$ (10 mM), and CTP (10 mM). After the addition of a CMP-sialic acid synthetase, the reaction was allowed to proceed for 6 h at 37 °C. The precipitates in the reaction mixture were removed by centrifugation and aliquots of 1 μL clear solution were diluted 100 times and injected for MS analysis.

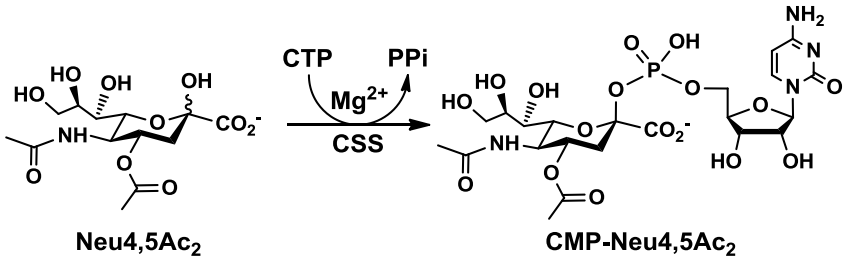

Molecular ion *m*/*z*: Neu5Ac, 308.0982; $Neu4,5Ac_2$, 350.1087;
CMP-Neu5Ac, 613.1394; $CMP\text{-}Neu4,5Ac_2$, 655.1500;
CTP, 481.9767; CDP, 402.0104; CMP, 322.0440

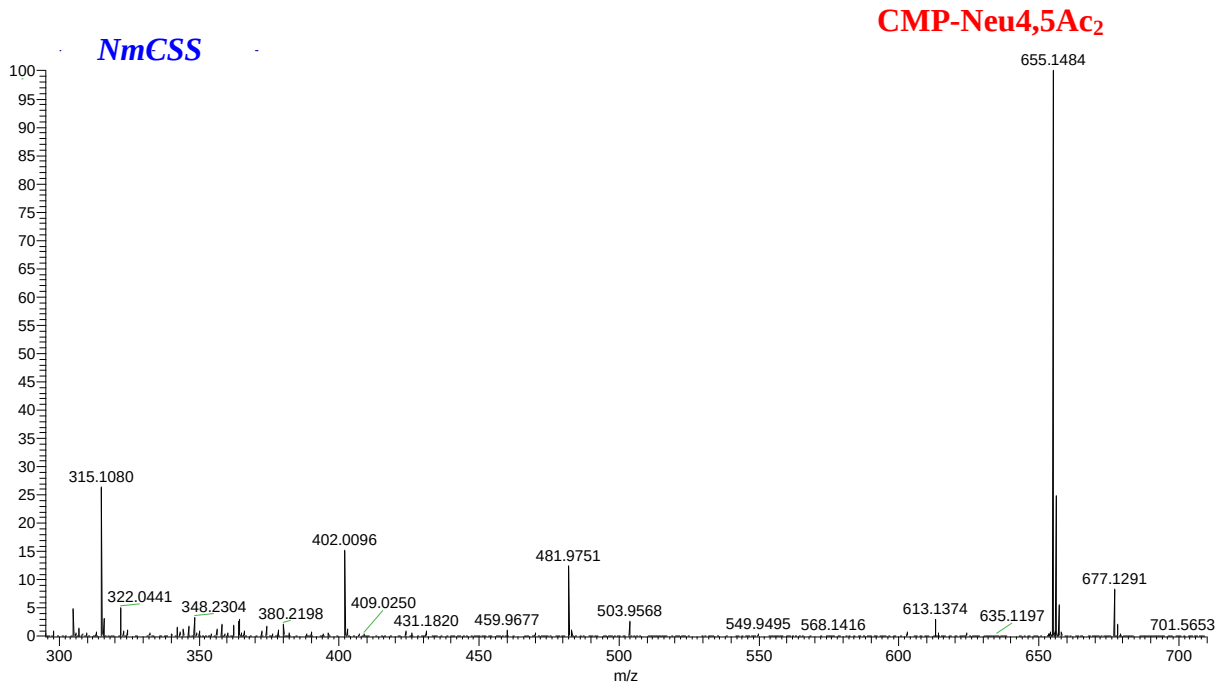

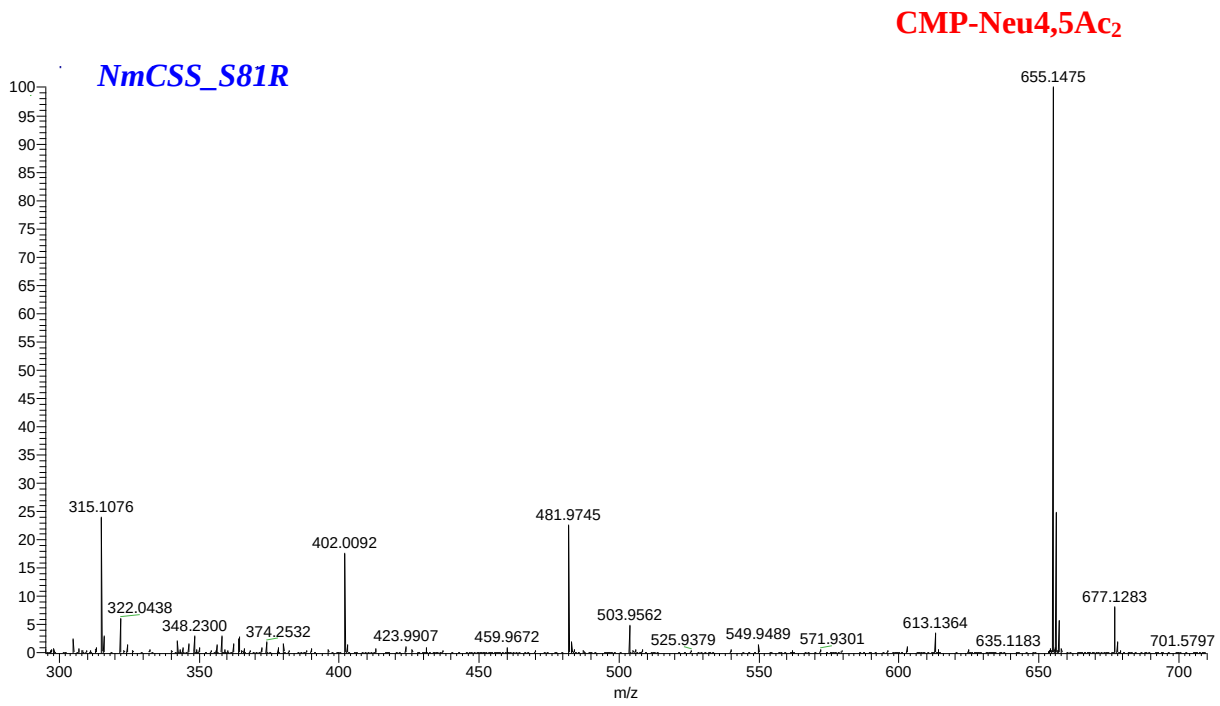
CMP-Neu4,5Ac2
NmCSS_S81R
655.1475
315.1076
481.9745
402.0092
322.0438
348.2300
374.2532
423.9907
459.9672
503.9562
525.9379
549.9489
571.9301
613.1364
635.1183
677.1283
701.5797
m/z

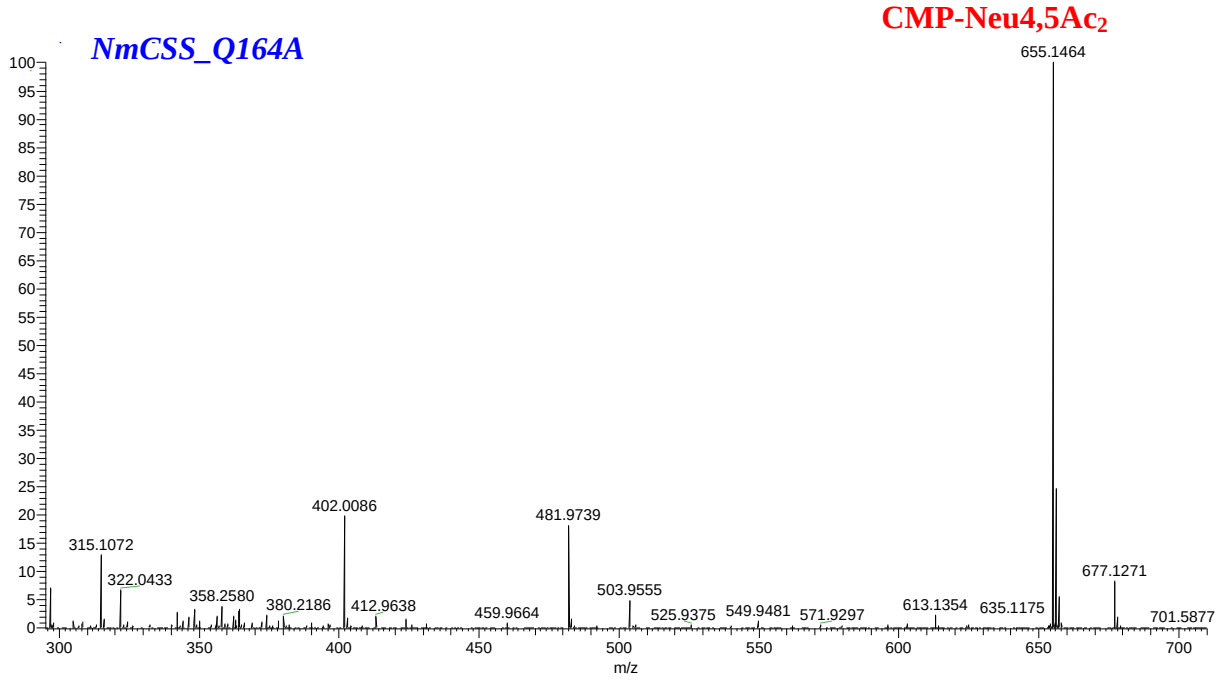
CMP-Neu4,5Ac2
NmCSS_Q164A
655.1464
315.1072
402.0086
481.9739
322.0433
358.2580
380.2186
412.9638
459.9664
503.9555
525.9375
549.9481
571.9297
613.1354
635.1175
677.1271
701.5877
m/z

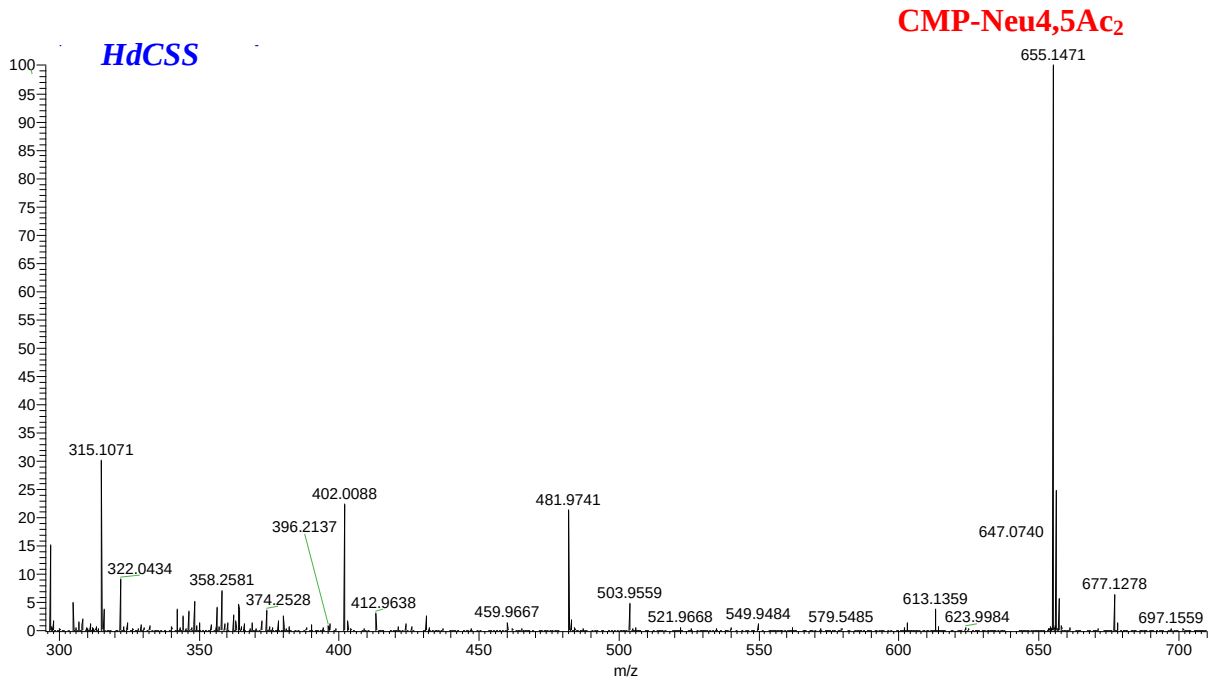
HdCSS
CMP-Neu4,5Ac2
655.1471
315.1071
402.0088
396.2137
481.9741
322.0434
358.2581
374.2528
412.9638
459.9667
503.9559
521.9668
549.9484
579.5485
613.1359
623.9984
647.0740
677.1278
697.1559
m/z

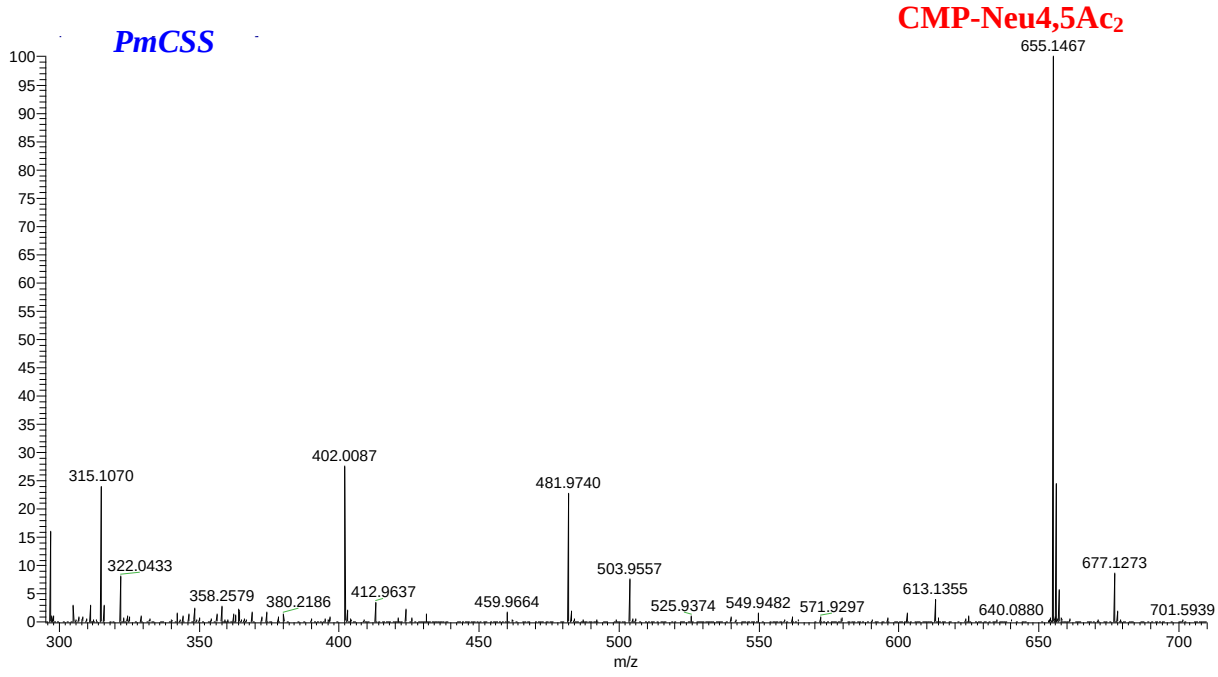
PmCSS
CMP-Neu4,5Ac2
655.1467
315.1070
402.0087
481.9740
322.0433
358.2579
380.2186
412.9637
459.9664
503.9557
525.9374
549.9482
571.9297
613.1355
640.0880
677.1273
701.5939
m/z

Fig. S2 Mass spectrometry (MS) chromatograms of human influenza virus neuraminidase-catalyzed hydrolysis of Neu4,5Ac$_2$α3Lac

A/Udorn/307/72 H3N2 (A/Udorn72)

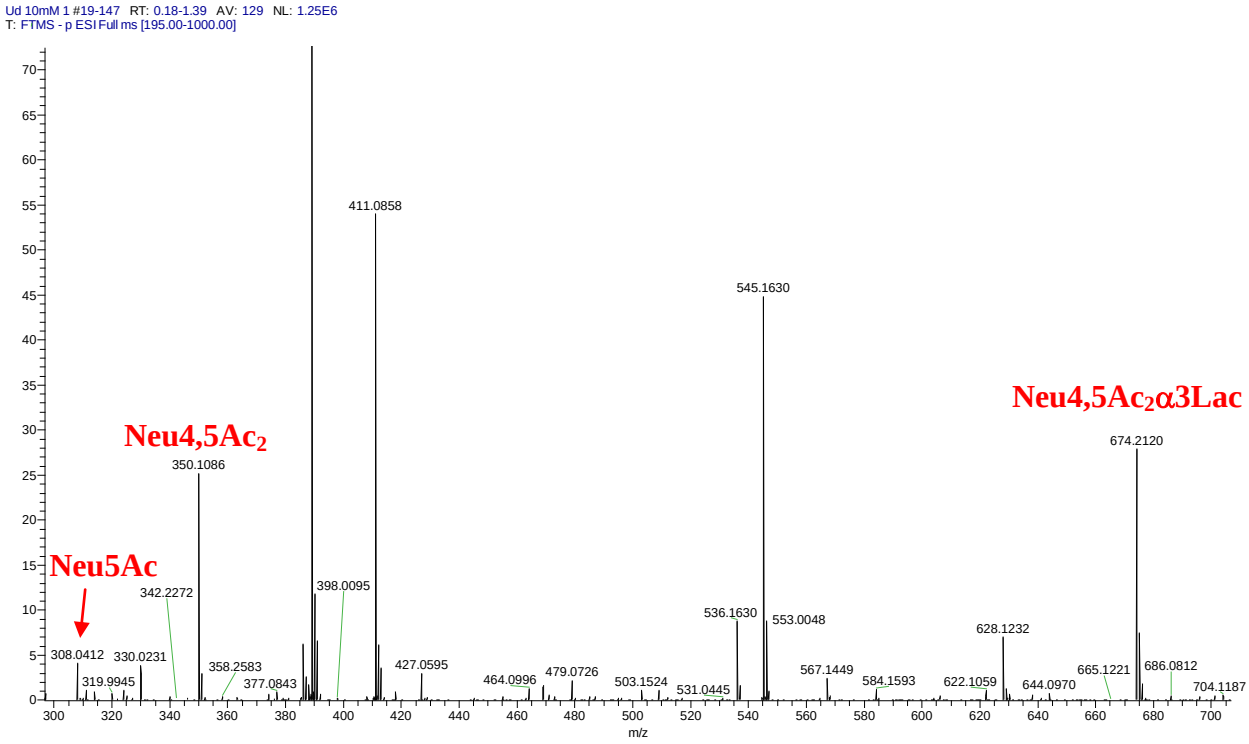

A/Memphis/71 H3N1 (A/Mem71)

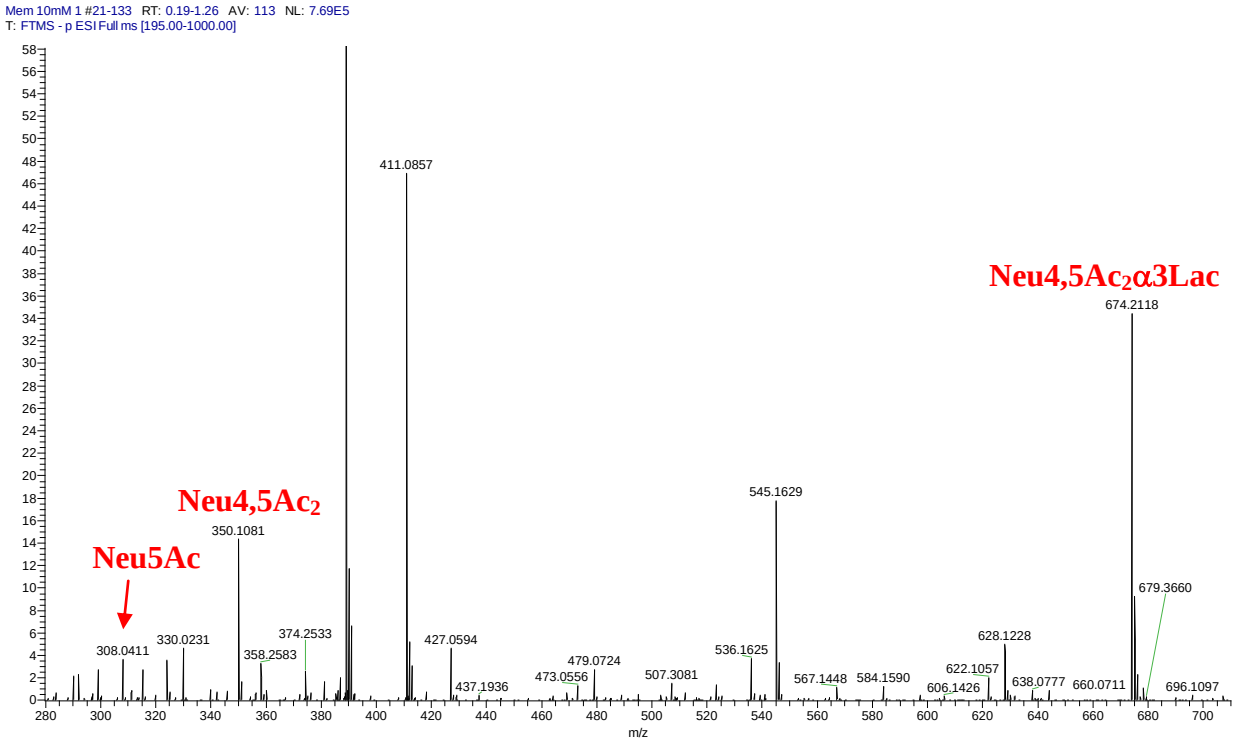

A/Puerto Rico/34/8 H1N1 (A/PR8)

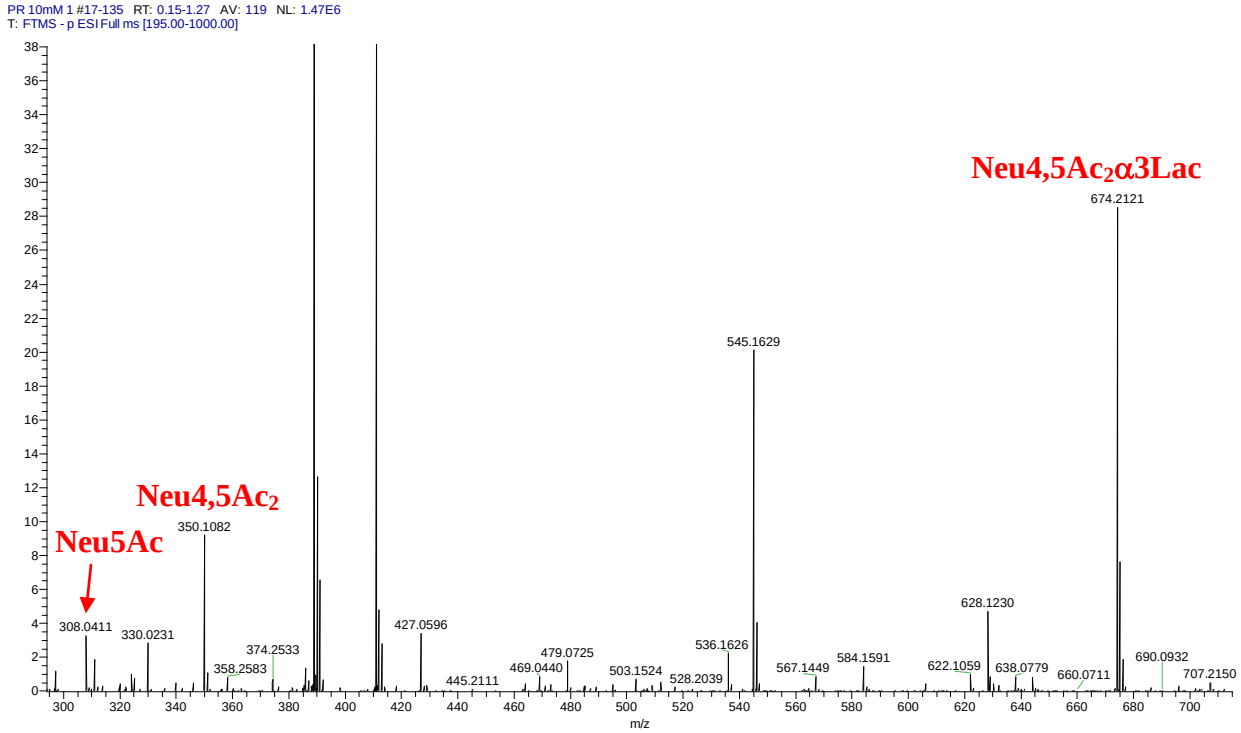

A/Philippines/2/82/X-79 H3N2 (A/Philips)

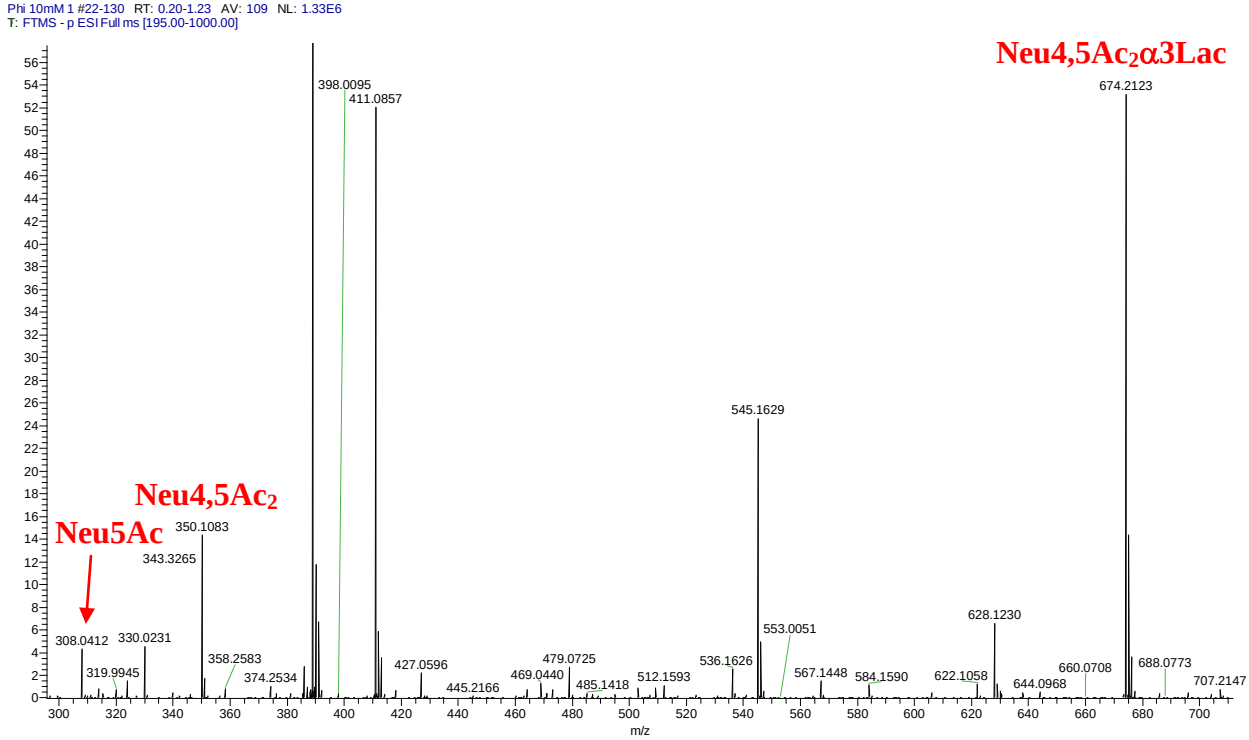

^{1}H and ^{13}C NMR spectra of Neu4,5Ac$_2$ (**1**)

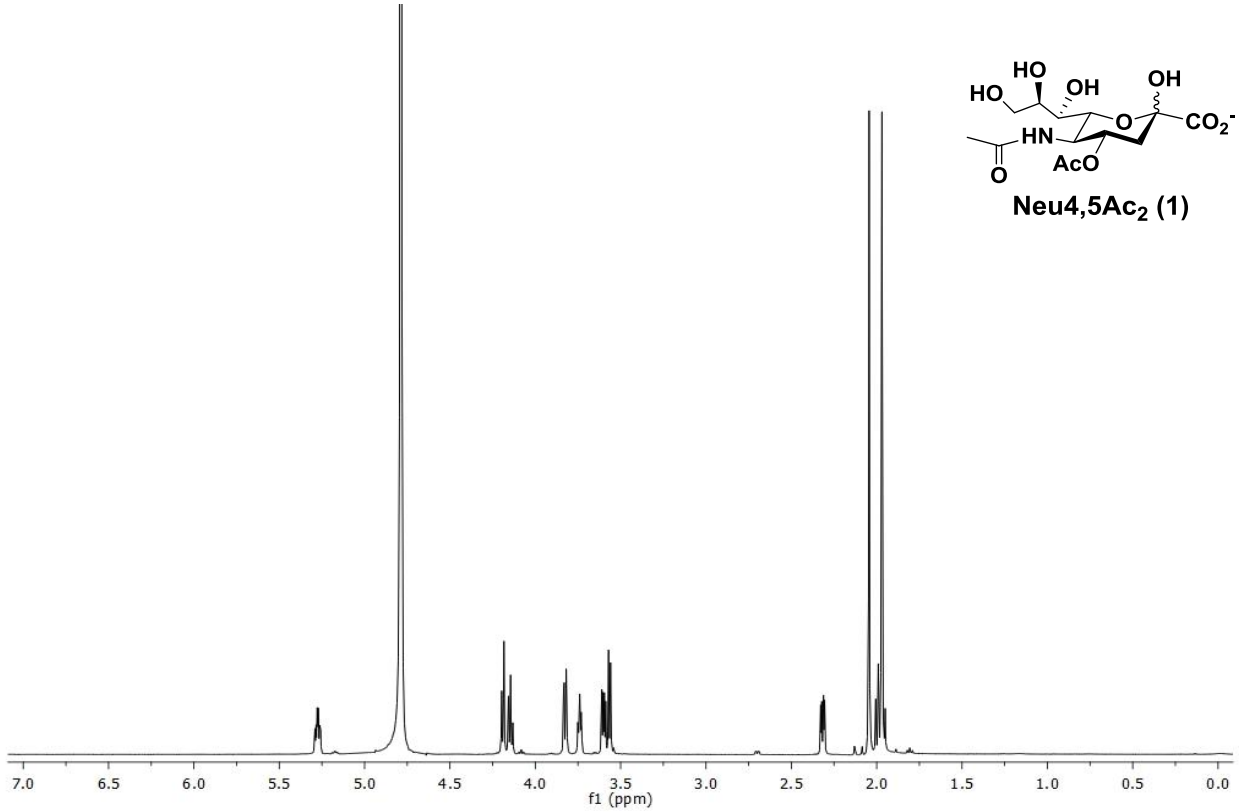

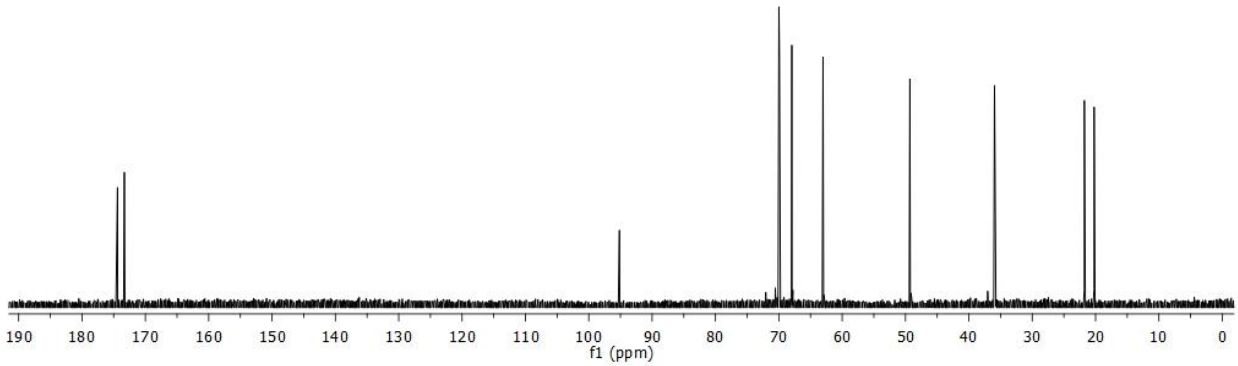

^{1}H and ^{13}C NMR spectra of Neu4Ac5Gc (**2**)

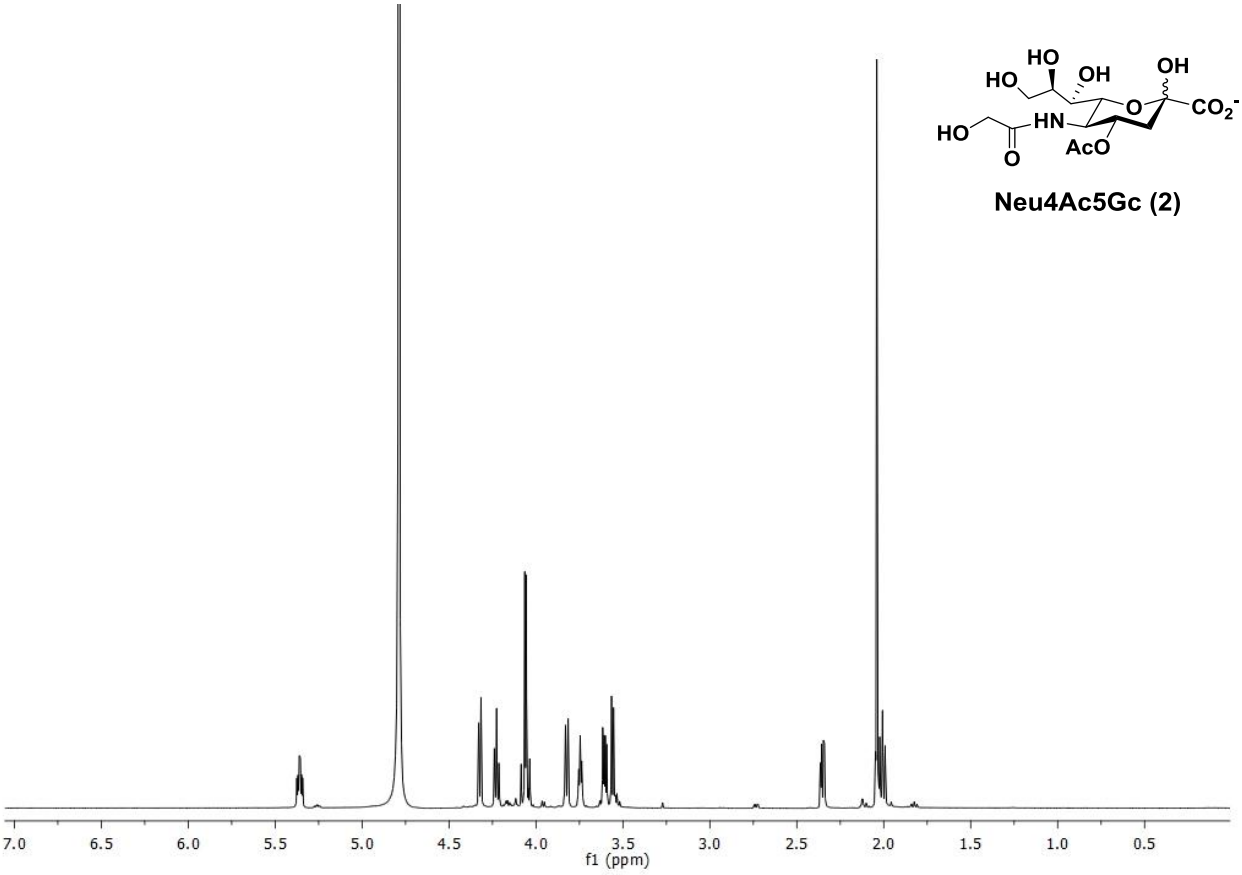

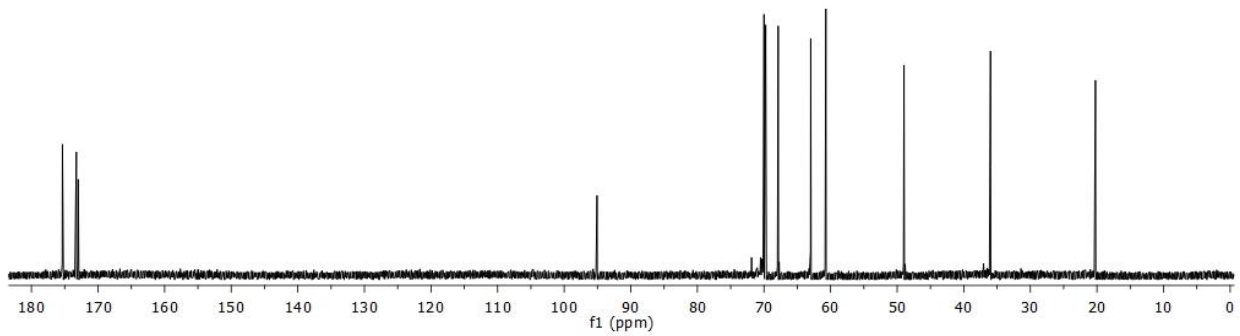

^{1}H and ^{13}C NMR spectra of GlcNAcβ3LacβProN_3 (Lc_3)

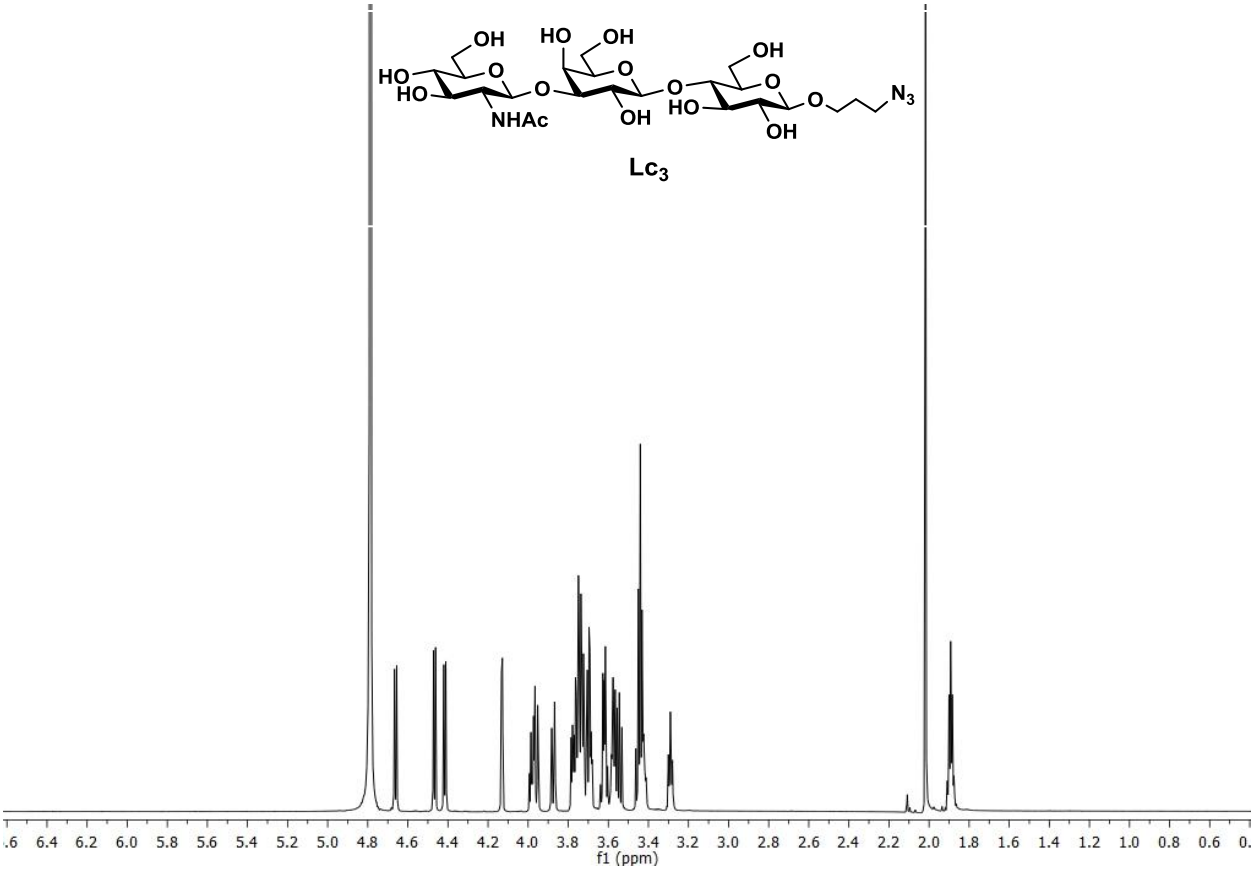

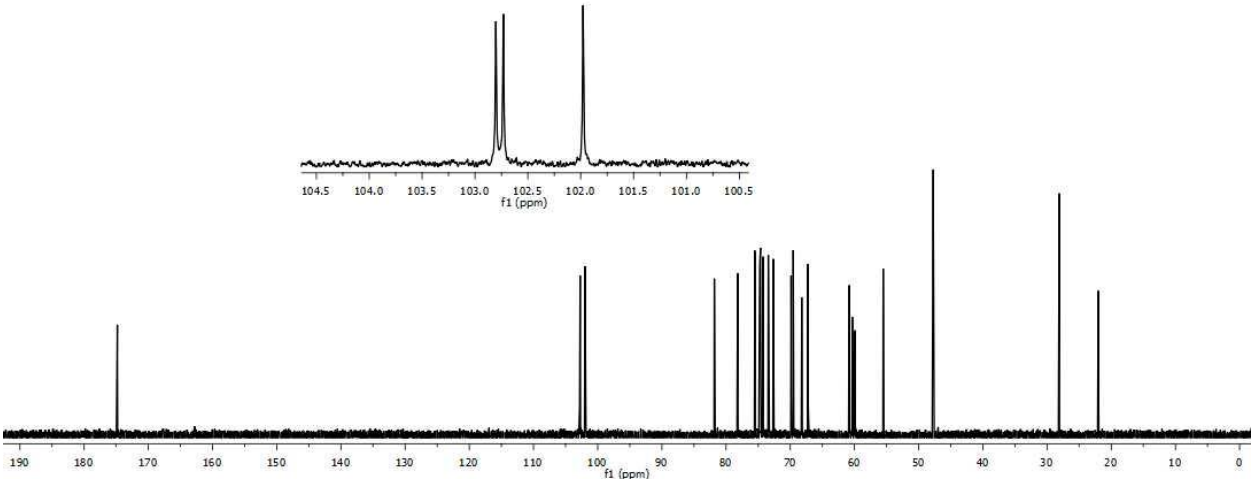

^{1}H and ^{13}C NMR spectra of LNnTβProN$_3$ (**23**)

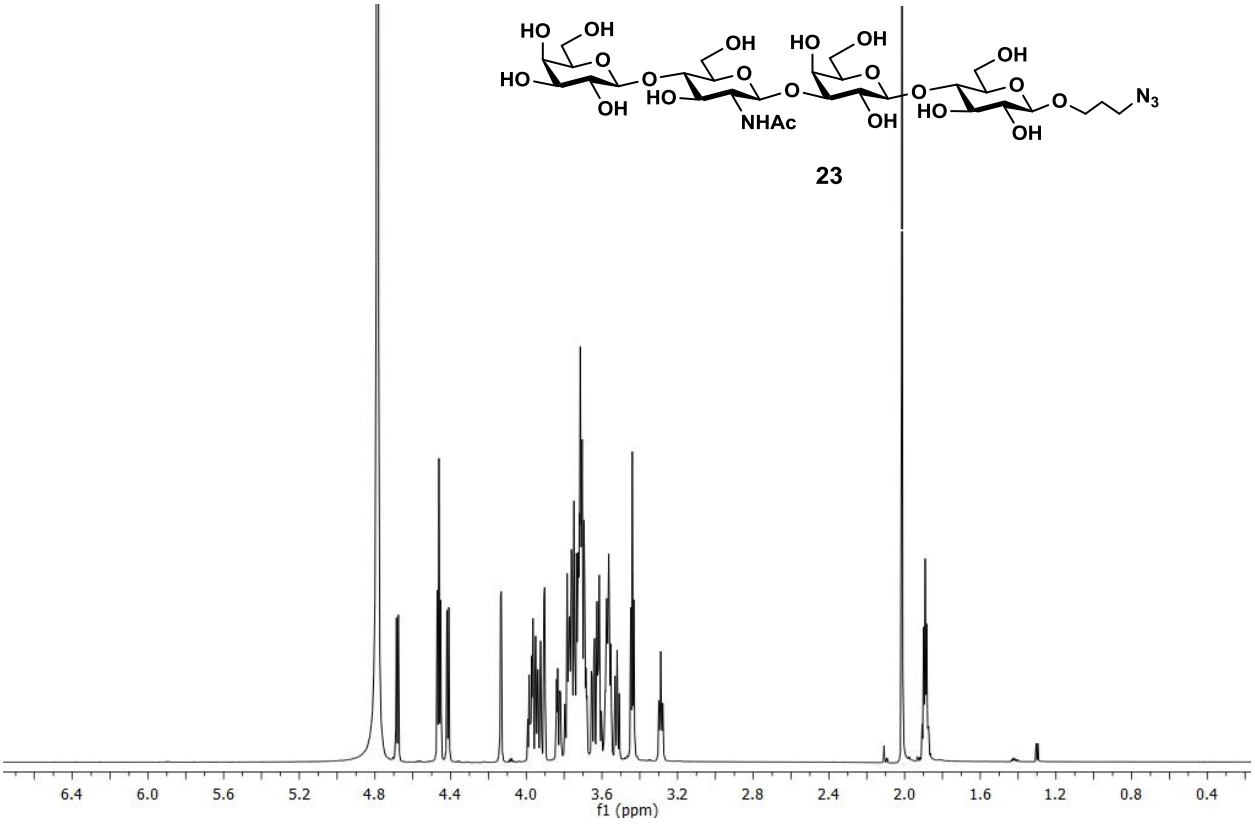

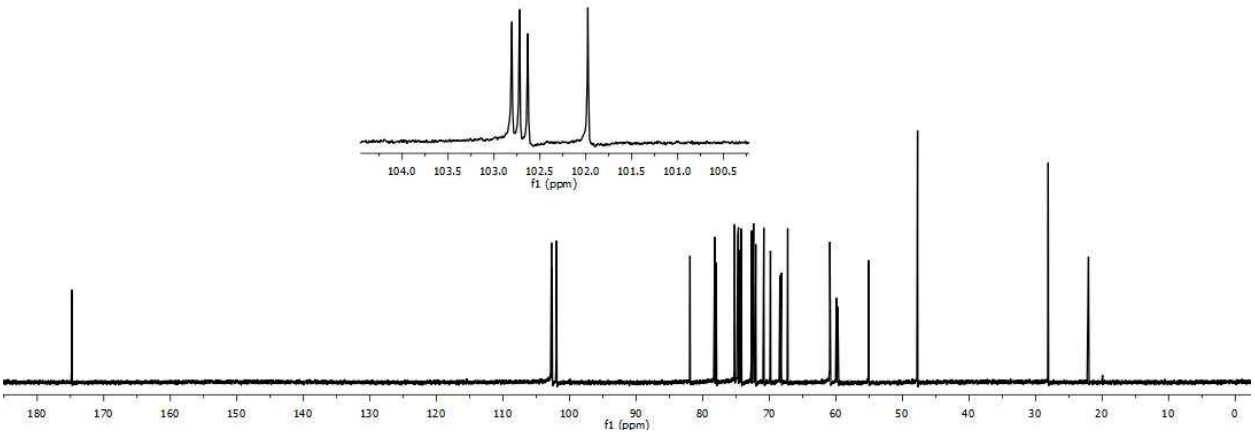

^{1}H and ^{13}C NMR spectra of Neu4,5Ac_2α3Lac (**24**)

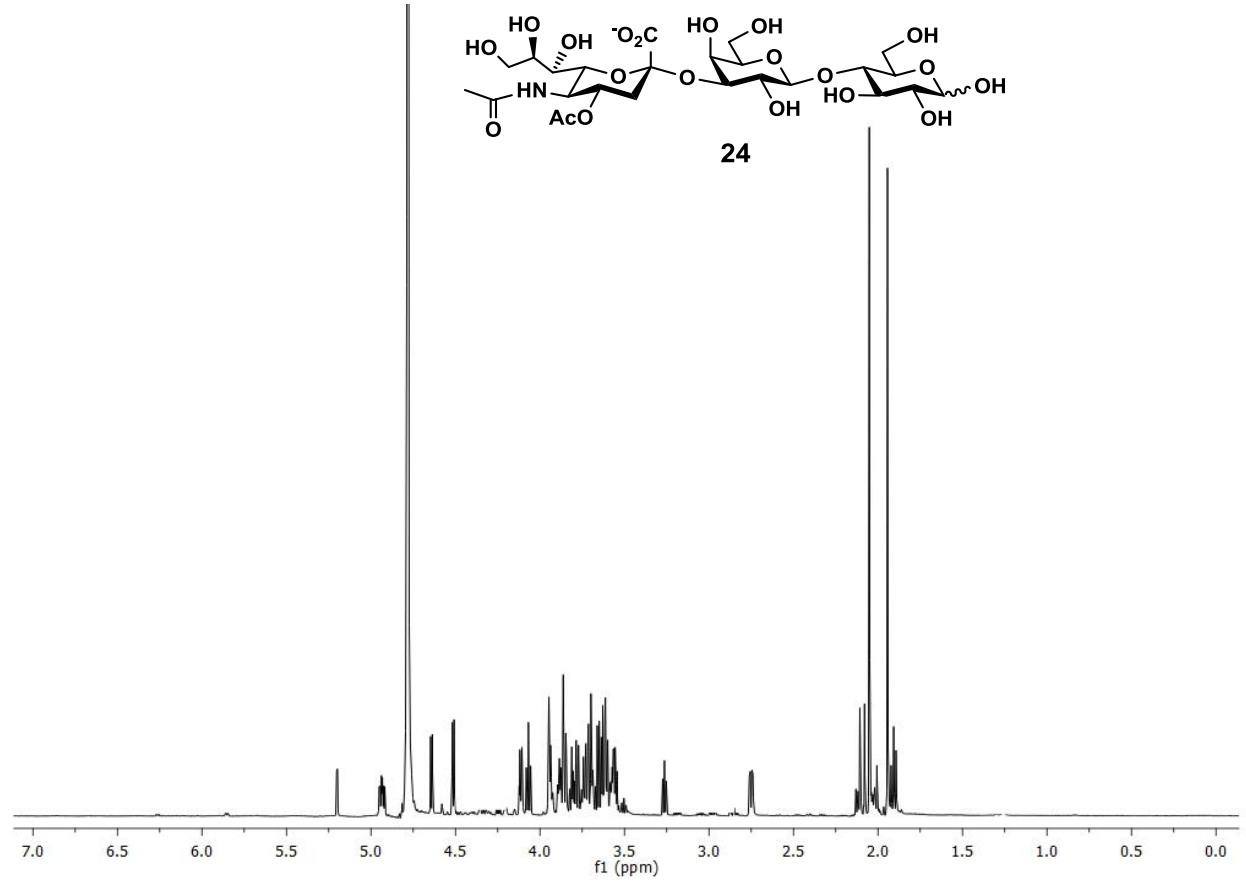

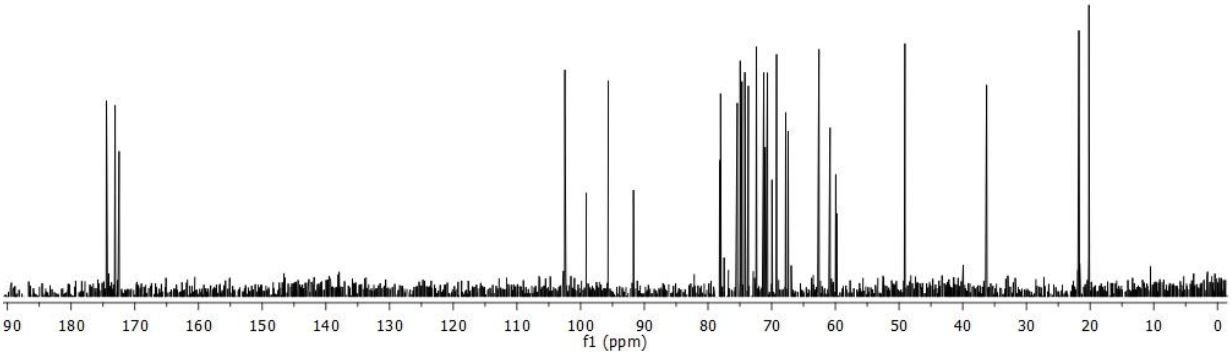

^{1}H and ^{13}C NMR spectra of Neu4,5Ac$_2$α3LNnT (**25**)

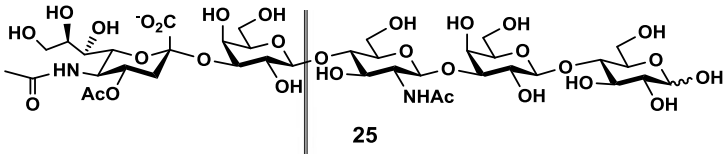

25

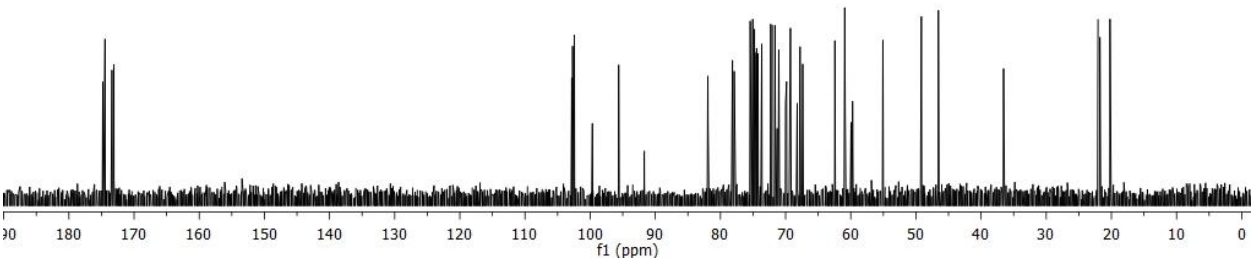

^{1}H and ^{13}C NMR spectra of Neu4,5Ac$_2$α3LNT (**26**)

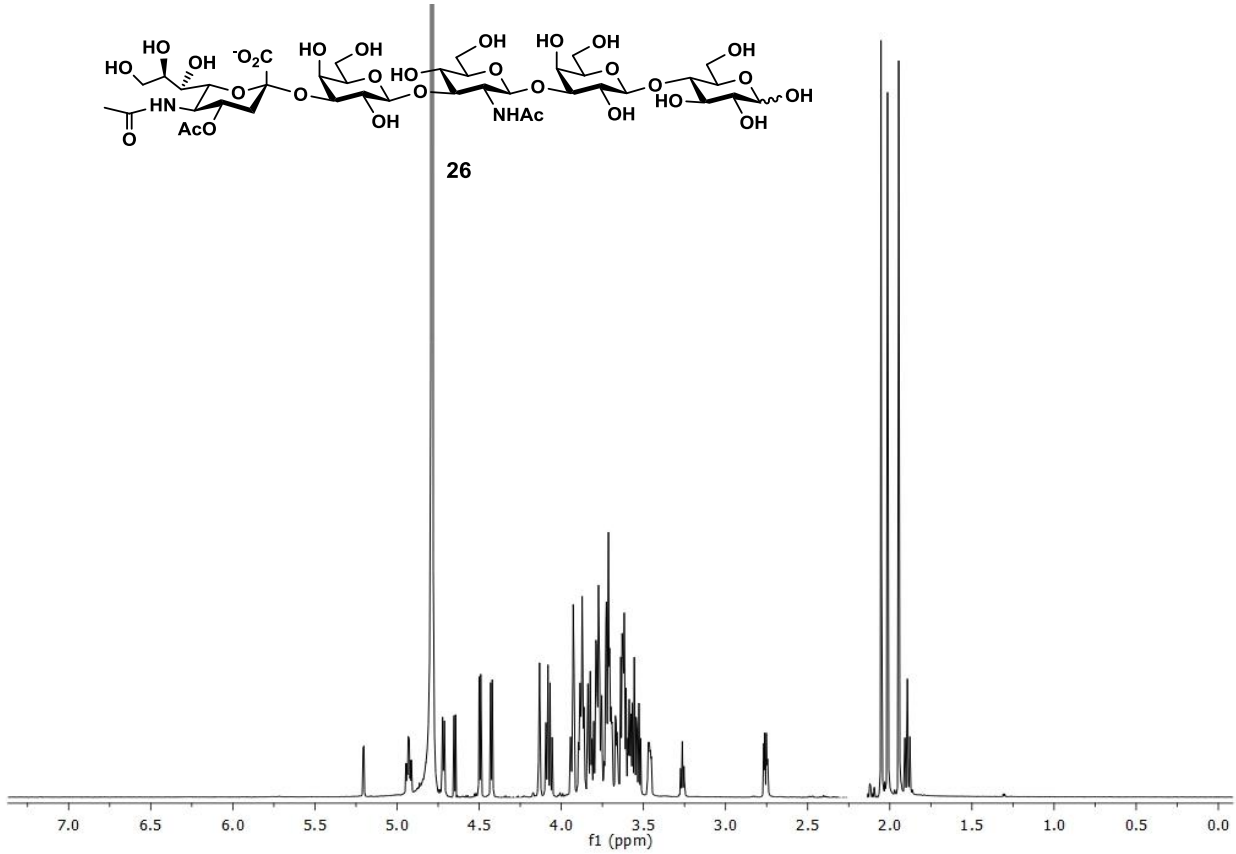

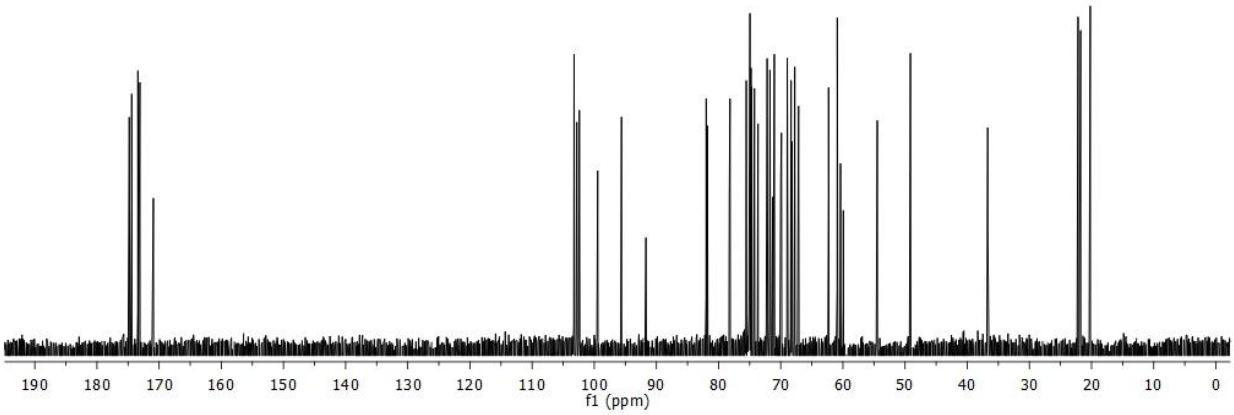

^{1}H and ^{13}C NMR spectra of Neu4,5Ac$_2$α3Galβ*p*NP (**27**)

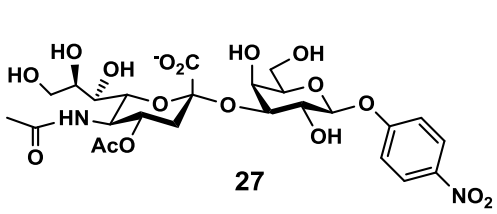

27

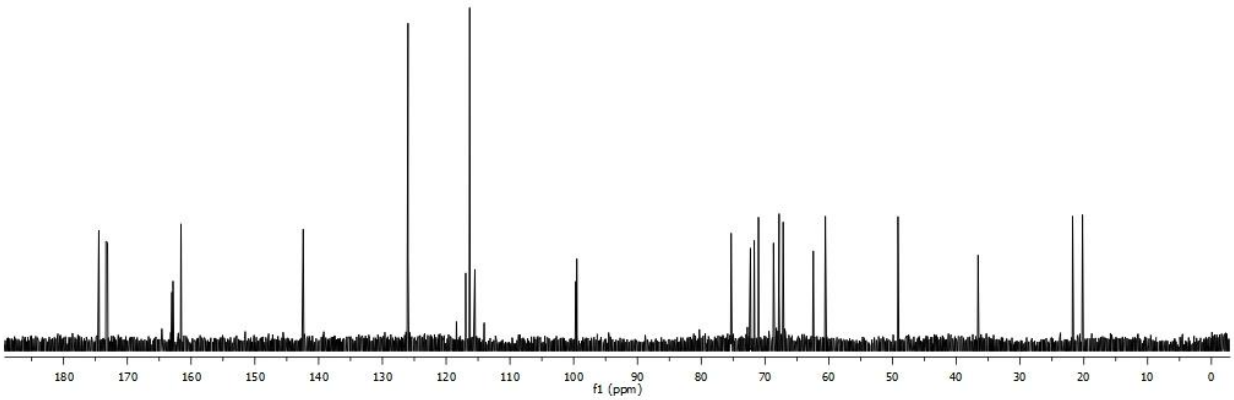

^{1}H and ^{13}C NMR spectra of Neu4,5Ac_2α3LacβProN_3 (**28**)

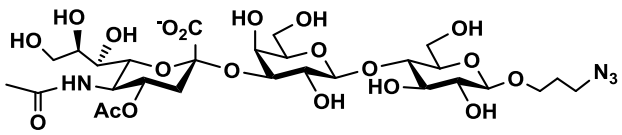

28

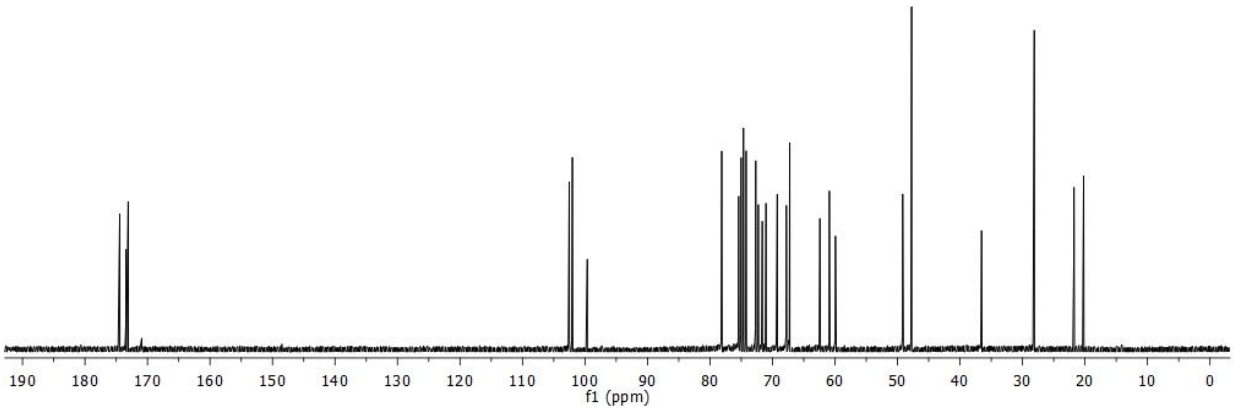

^{1}H and ^{13}C NMR spectra of Neu4,5Ac_2α3LacNAcβProN_3 (**29**)

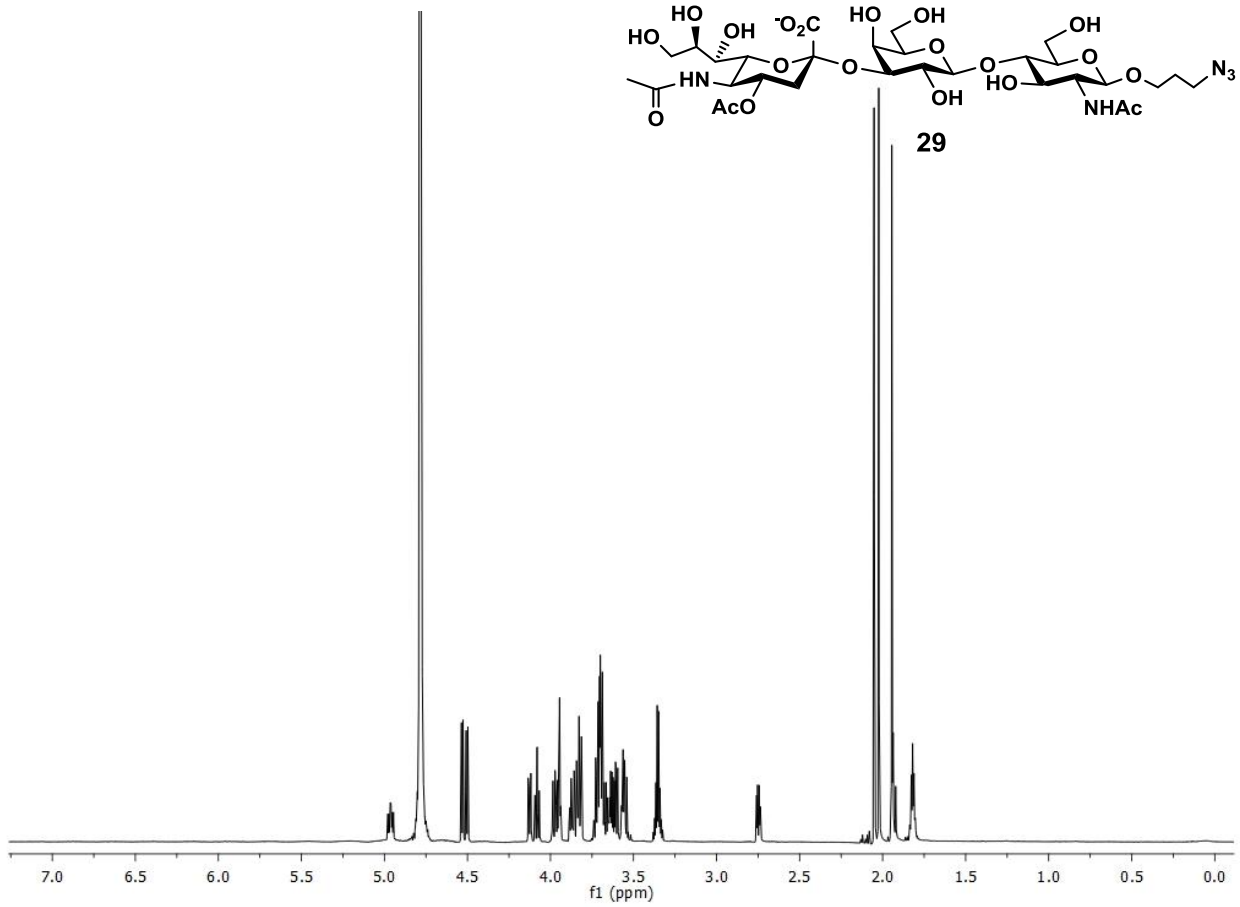

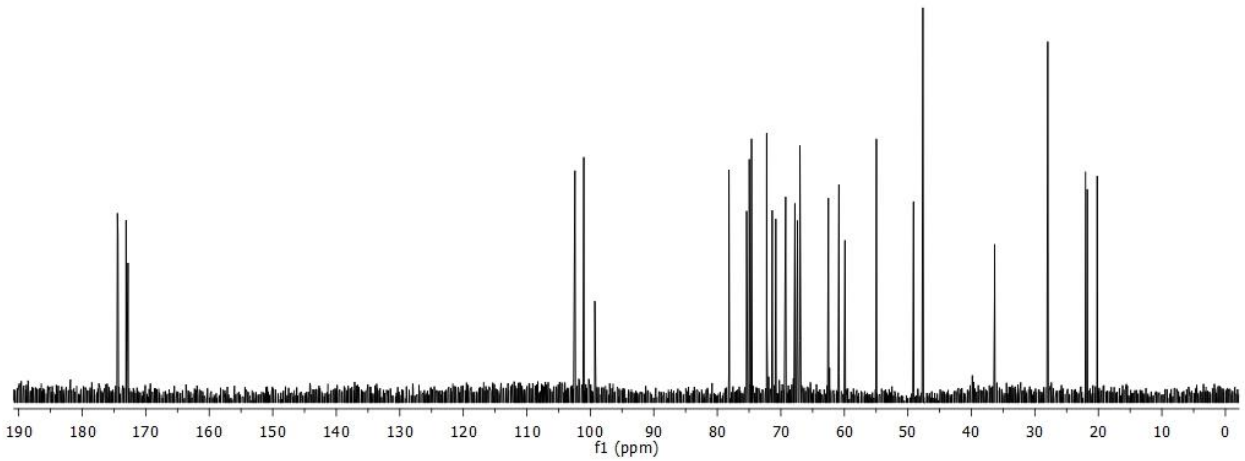

^{1}H and ^{13}C NMR spectra of Neu4,5Ac_2α3Galβ3GlcNAcβProN_3 (**30**)

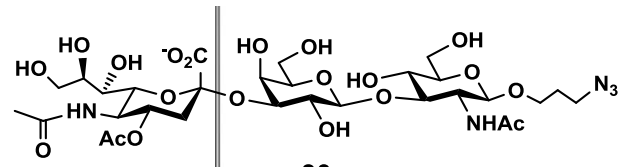

30

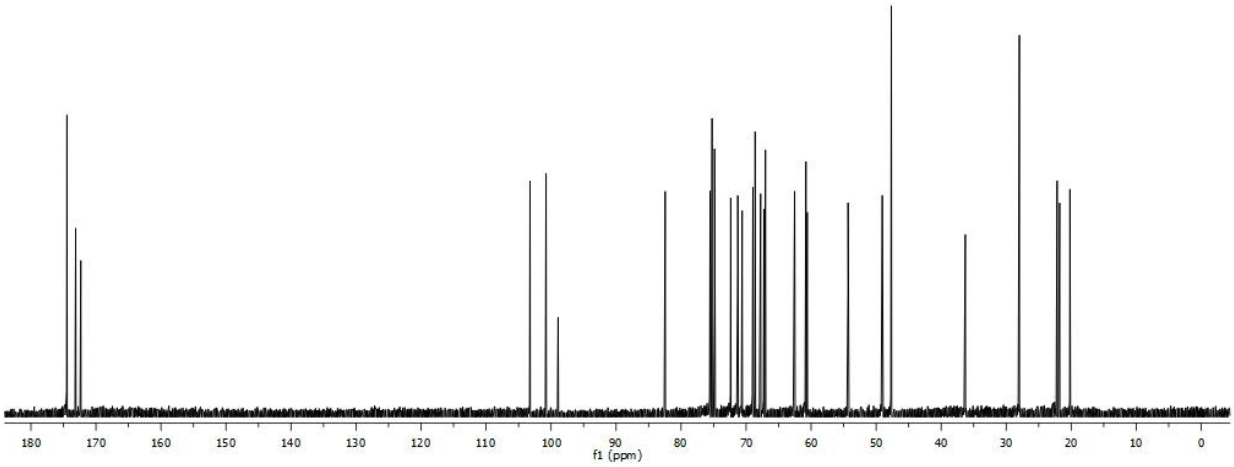

^{1}H and ^{13}C NMR spectra of Neu4,5Ac$_2$α3Galβ3GlcNAcαProN$_3$ (**31**)

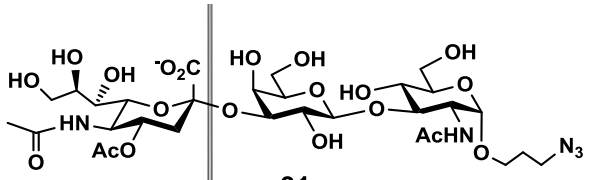

31

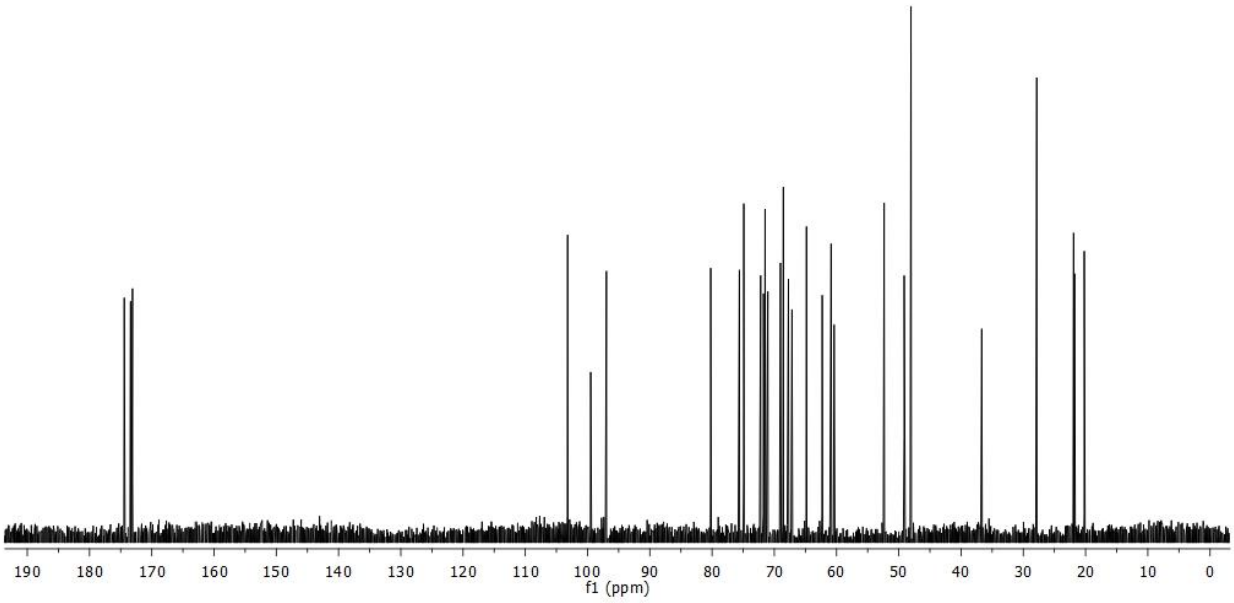

^{1}H and ^{13}C NMR spectra of Neu4,5Ac$_2$α3Galβ3GalNAcβProN$_3$ (**32**)

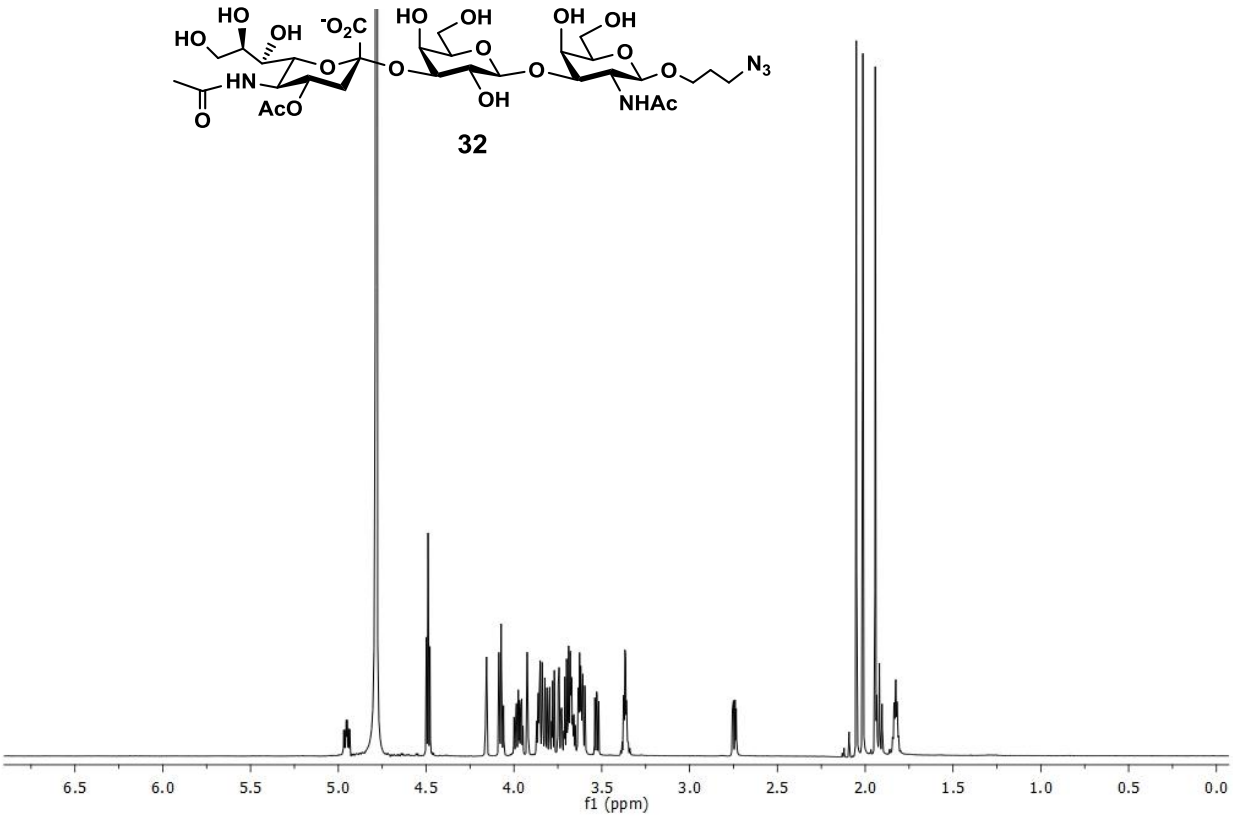

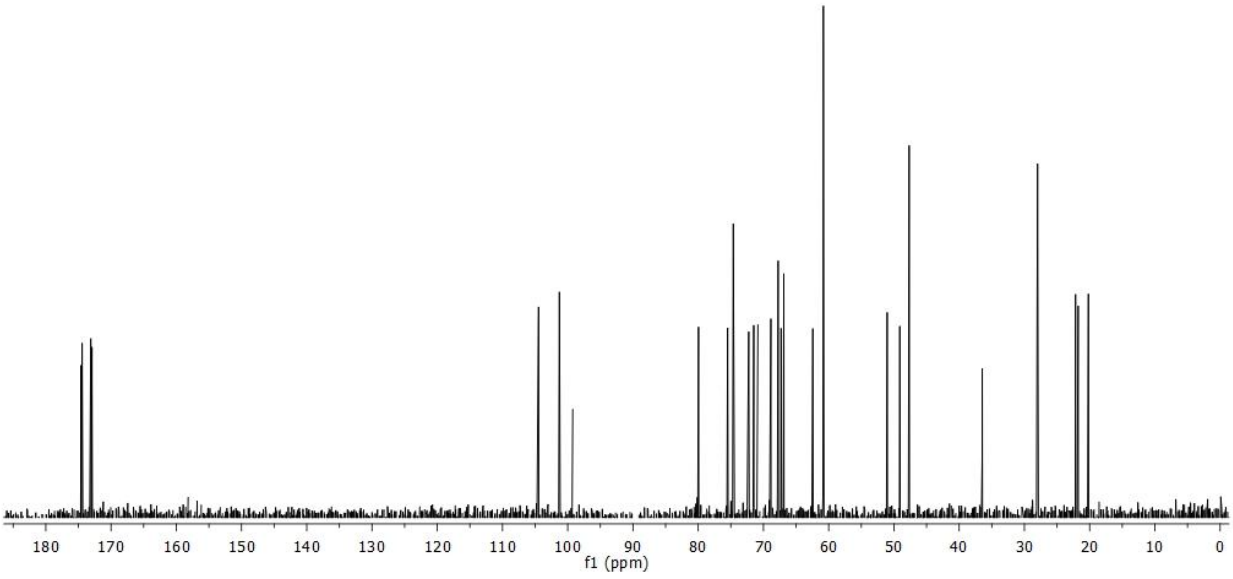

^{1}H and ^{13}C NMR spectra of Neu4,5Ac$_2$α3Galβ3GalNAcαProN$_3$ (**33**)

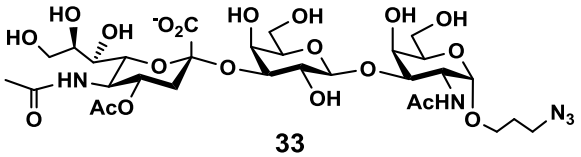

33

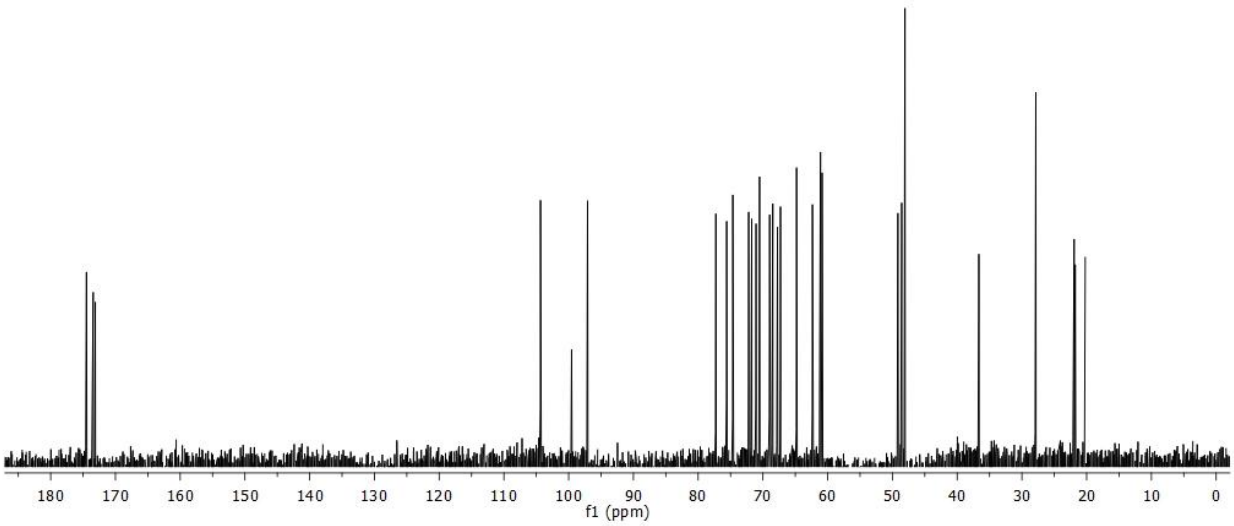

^{1}H and ^{13}C NMR spectra of Neu4,5Ac$_2$α3LNnTβProN$_3$ (**34**)

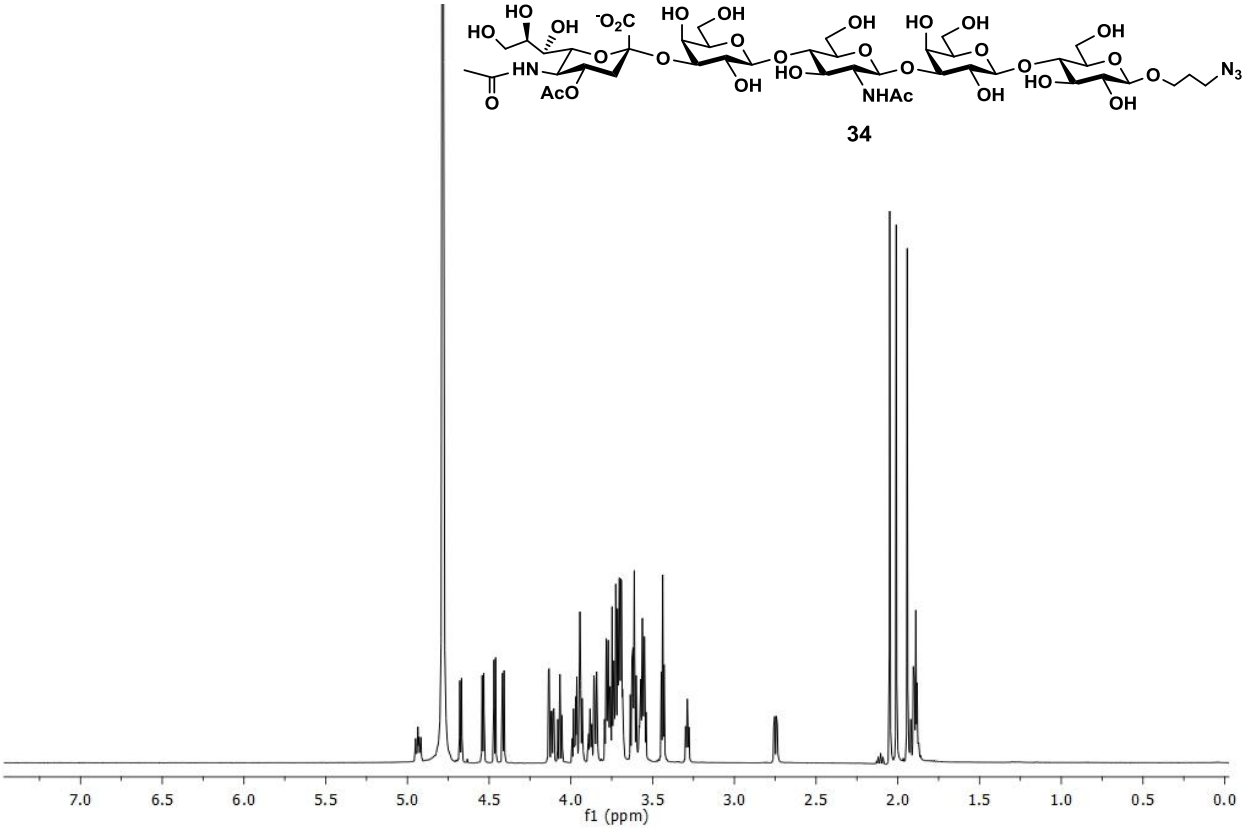

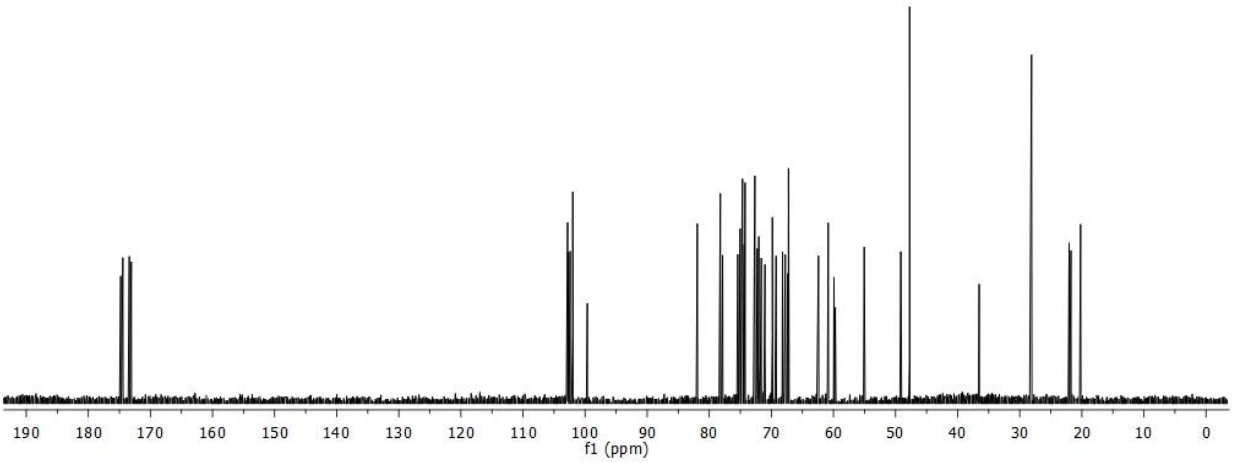

^{1}H and ^{13}C NMR spectra of Neu4Ac5Gcα3LacβProN_3 (**35**)

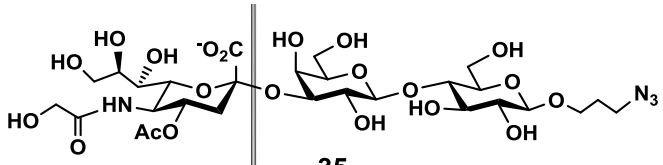

35

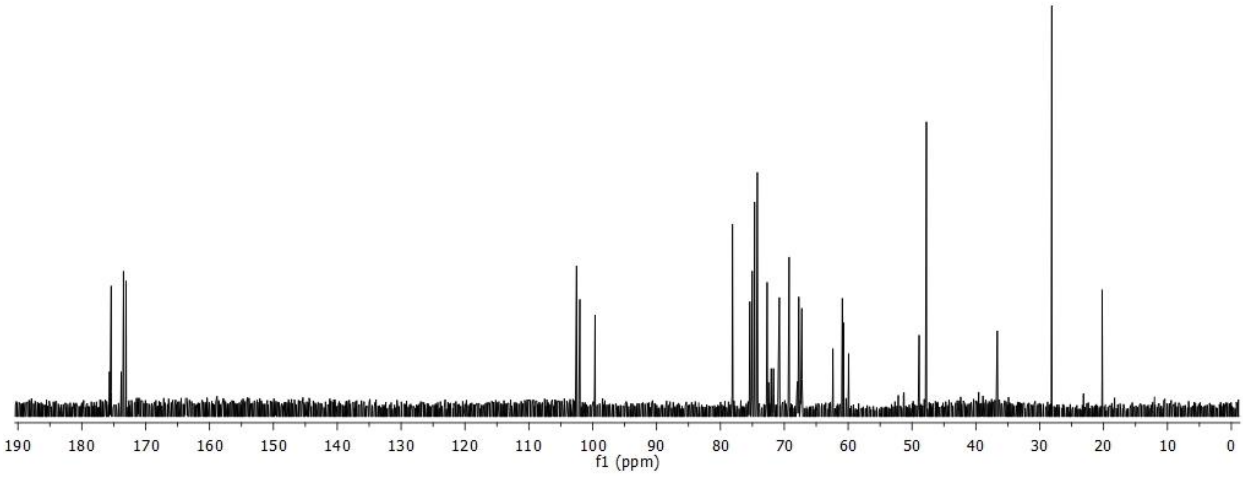

^{1}H and ^{13}C NMR spectra of Neu4Ac5Gcα3LacNAcβProN_3 (**36**)

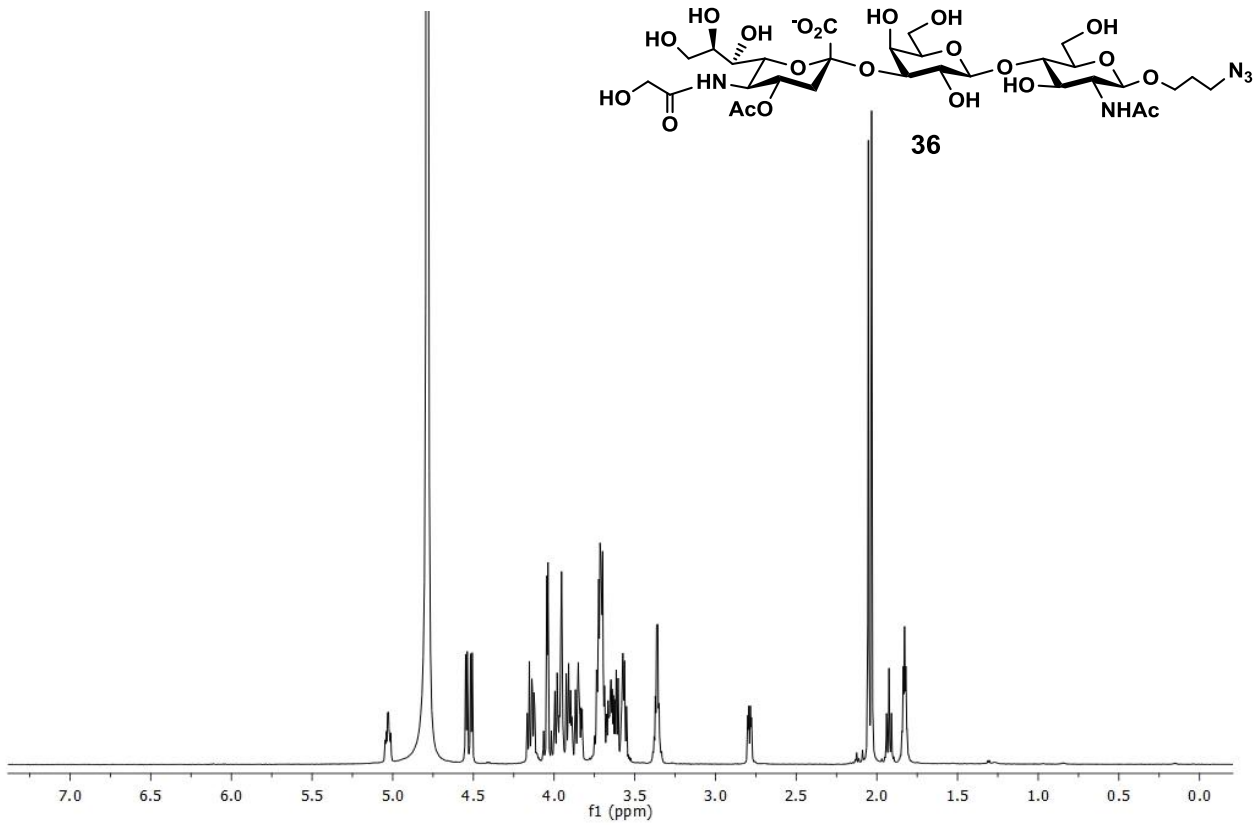

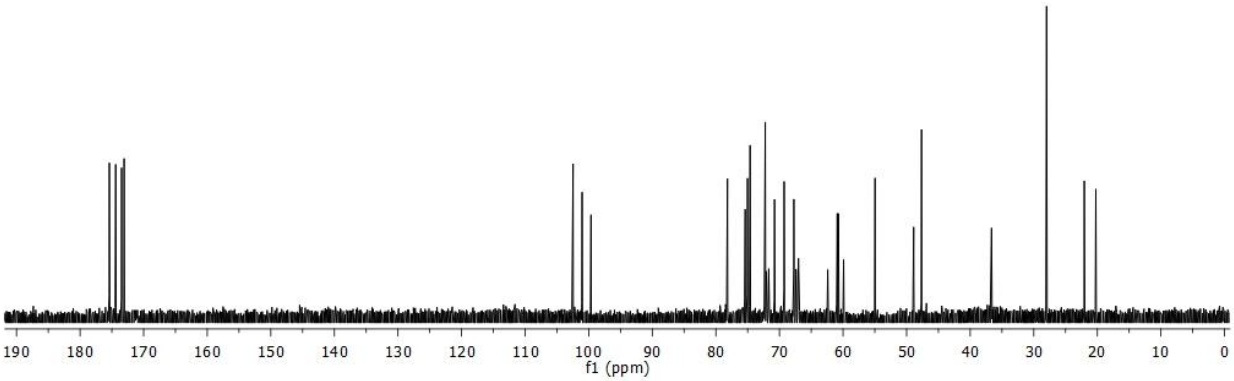

^{1}H and ^{13}C NMR spectra of Neu4Ac5Gcα3Galβ3GlcNAcβProN_3 (**37**)

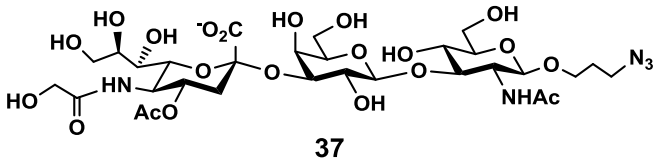

37

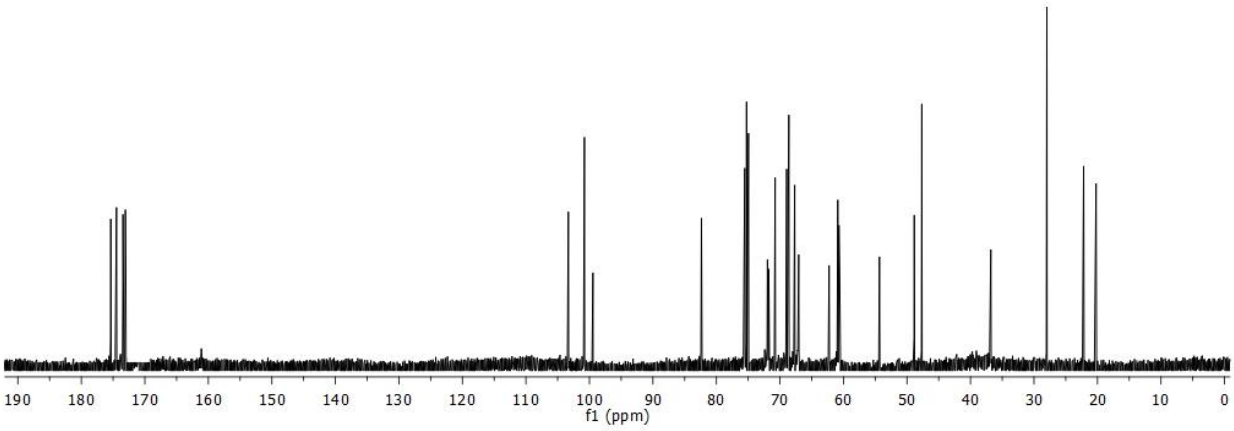

^{1}H and ^{13}C NMR spectra of Neu4Ac5Gcα3Galβ3GlcNAcαProN_3 (**38**)

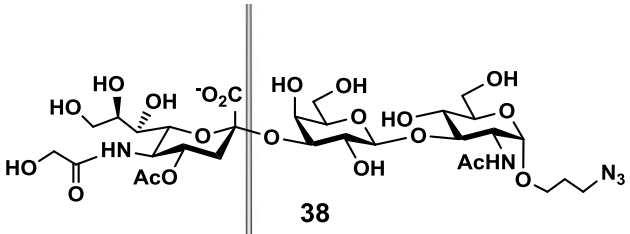

38

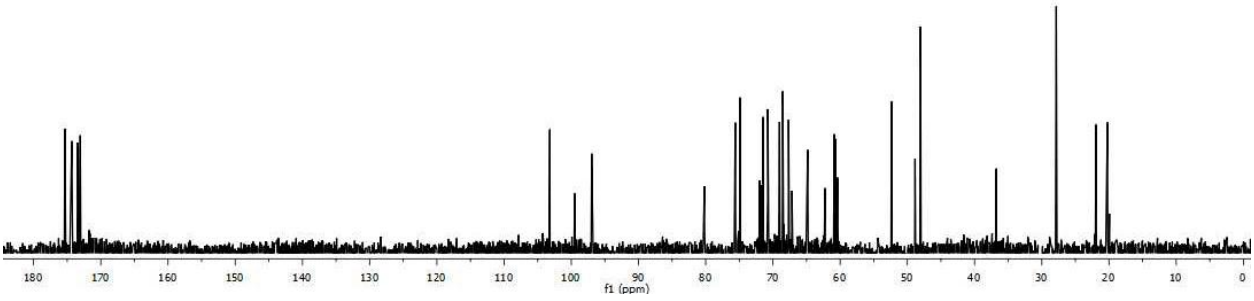

^{1}H and ^{13}C NMR spectra of Neu4Ac5Gcα3Galβ3GalNAcβProN_3 (**39**)

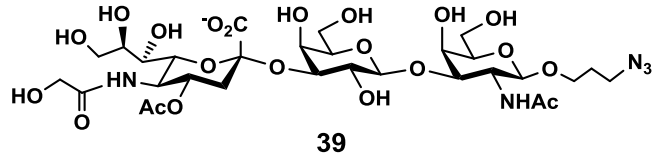

39

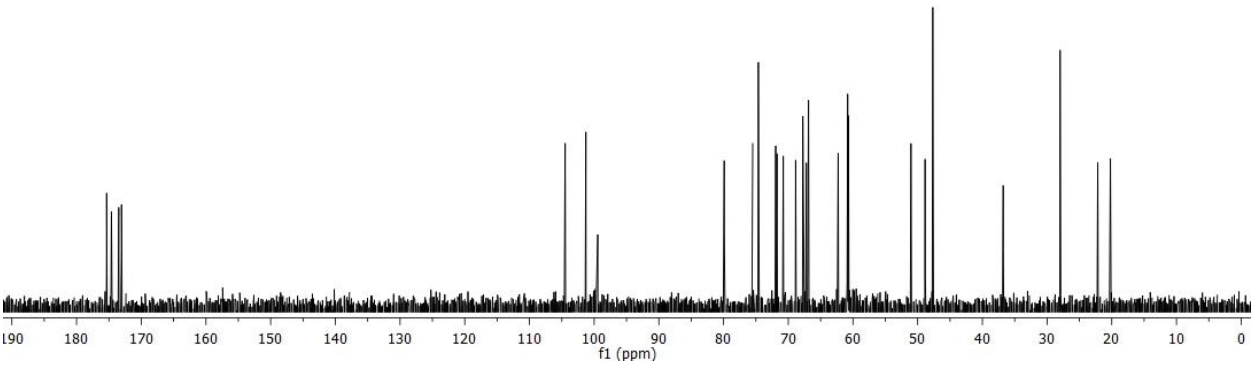

^{1}H and ^{13}C NMR spectra of Neu4Ac5Gcα3Galβ3GalNAcαProN_3 (**40**)

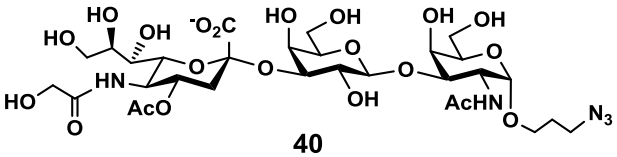

40

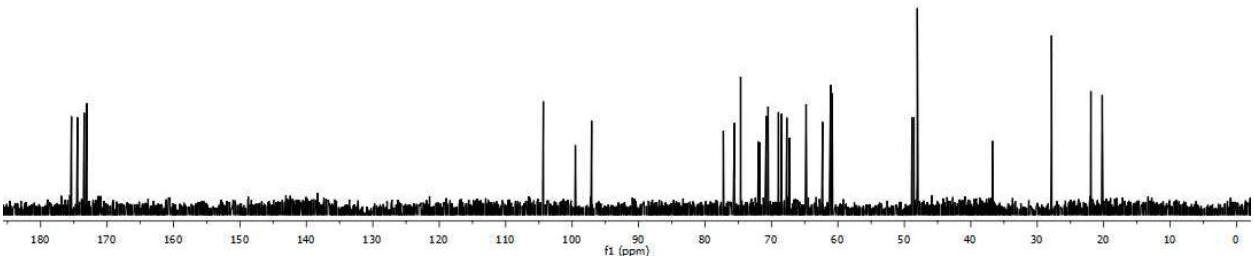

^{1}H and ^{13}C NMR spectra of Neu4Ac5Gcα3LNnTβProN$_3$ (**41**)

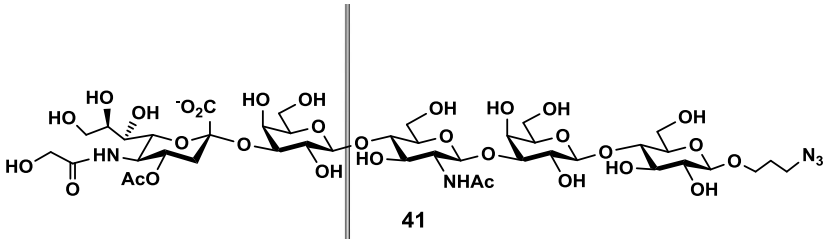

41